Local and Microdomain Concentration Fluctuation Effects in Block Copolymer Solutions

Marina Guenza† and Kenneth S. Schweizer*

Departments of Materials Science & Engineering and Chemistry and Materials Research Laboratory, University of Illinois, 1304 West Green Street, Urbana, Illinois 61801

Received February 6, 1997; Revised Manuscript Received May 8, 1997[⊗]

ABSTRACT: On the basis of the simplest Gaussian thread model for structurally symmetric copolymers, the polymer reference interaction site model (PRISM) theory is applied to study the equilibrium properties of diblock copolymer solutions under neutral solvent conditions. Analytic predictions are obtained for the influence of local and microdomain scale concentration fluctuations on the relationship between temperature, degree of polymerization, and polymer concentration at the order−disorder transition (ODT). In the semidilute regime, PRISM predictions agree with blob scaling and fluctuation-corrected field theoretic analyses. However, in the concentrated solution and melt regime strong disagreements occur, and the naive mean field dilution approximation is found to fail. Nevertheless, apparent scaling laws emerge under concentrated conditions with effective exponents which depend on solvent quality, melt screening length, and other nonuniversal structural features. The primary origin of the dilution approximation failure is interchain nonrandom mixing, which is concentration dependent and driven by local packing effects. Microdomain scale fluctuations yield corrections of secondary importance which vanish in the long chain limit. For concentrated solutions and good solvents, the predicted apparent exponent is fortuitously in close agreement with semidilute blob scaling results, and also agrees with recent measurements on polystyrene−polyisoprene diblocks by Lodge and co-workers. Smaller effective exponents are found under Θ solvent conditions. Systematic PRISM model calculations for properties strongly affected by microdomain scale fluctuations, such as small angle scattering intensity and local physical clustering, are also presented. Significant physical clustering is found in solutions of compositionally asymmetric diblocks even very far from the ODT.

I. Introduction

Much experimental and theoretical progress has been made in recent years in understanding the structure and thermodynamic behavior of self-assembling diblock copolymer melts.[1] Issues of primary concern include the role of long wavelength (microdomain scale) concentration fluctuations, novel ordered microstructures, and the influence of system-specific features such as "conformational asymmetry" on the location and shape of order−disorder transition (ODT) boundaries. The subject of the present paper is the disordered (but highly fluctuating) phase and the ODT condition for diblock copolymer fluids and not the symmetry and structure of the ordered microphases. For these questions, significant theoretical advances have been made for diblock melts following two very different approaches.

The first approach is field theory for highly coarse-grained models based on Landau expansions of an effective free energy,[2] ideal Gaussian chain statistics,[3] the random phase approximation (RPA),[4] and an incompressibility constraint. Leibler[5] developed the seminal mean field theory (MFT), and Fredrickson and Helfand[6] approximately included microdomain scale concentration fluctuation corrections following the method of Brazovskii.[7] We shall refer to the latter approach as the BLFH theory. Recently, Stepanow[8] has generalized the incompressible field theory beyond the RPA and has found major modifications of the BLFH theory.

An entirely different, microscopic liquid state integral equation theory for diblock copolymer fluids has been developed by David and Schweizer[9,10] based on "polymer reference interaction site model" (PRISM) methods.[11] Besides the inevitable differences between any approach formulated at the level of coarse-grained fields and a microscopic theory, PRISM is distinguished from the BLFH theory in additional ways. These include the incorporation of nonzero compressibility (and hence a nonzero density screening length), explicit treatment of (system-specific) intra- and intermolecular site−site pair potentials and correlations, no obvious restriction to very large degree of polymerization N, and a fundamentally different origin of the concentration fluctuation feedback effects which stabilize the disordered phase and destroy all critical and spinodal divergences. The predictions for BLFH and PRISM have been recently compared in depth, and quantitative tests of the ability of these theories to describe small angle scattering data in melts has also been carried out.[12] Both theories can accurately fit melt data sets, and under some conditions (nearly symmetric composition, high copolymer densities, moderate temperatures, large N), there are striking mathematical similarities between the microdomain scale predictions of the two different theories. However, for strongly asymmetric compositions, short chains, compressible copolymer solutions, and/or low temperatures, many significant differences emerge which have experimentally observable consequences.[12]

The goal of the present paper is to work out the predictions of PRISM theory for the simplest conceivable model of compressible AB diblock copolymer solutions under neutral (nonselective) solvent conditions. Solutions of copolymers have been studied far less than melts,[13−21] and are more poorly understood. The reasons for this are the new physical complications which arise in solution such as enhanced polymer fluctuations associated with the increased (osmotic) compressibility of the copolymer subsystem, concentration dependent chain swelling due to unscreened excluded volume interactions in good solvents, and strong modification

† Permanent Address: Istituto di Studi Chimico-Fisici di Macromolecole Sintetiche e Naturali, IMAG, National Research Council, Via de Marini 6, Genova, Italy.

⊗ Abstract published in *Advance ACS Abstracts,* July 1, 1997.

S0024-9297(97)00173-3 CCC: $14.00

of the local interchain pair correlations due to entropic packing effects. Many of these same physical issues arise for other systems such as homopolymer solutions, binary blend solutions, solutions of AB multiblock copolymers, and perhaps polymer melts subjected to external pressure. Copolymer solutions are also of practical importance since dilution with a nonselective solvent can shift the ODT into experimentally accessible windows of temperature and/or degree of polymerization, and copolymer films are often solution cast by various processing protocols.

Besides the general motivations for studying copolymer solutions mentioned above, several recent experimental studies[19,20] are particularly puzzling and provide specific motivation for our theoretical work. Lodge and co-workers[19] have shown that the so-called "dilution approximation", which states that the degree of polymerization at the (constant temperature) ODT, N_{ODT}, is inversely proportional to the copolymer volume fraction in solution, $N_{ODT} \propto \phi^{-1}$, fails for styrene−isoprene (PS−PI) and a polyolefin diblock even under concentrated solution conditions. The manner in which it fails is particularly provocative. For PS−PI solutions a scaling law is found: $\phi_{ODT} \propto N^{-0.62}$ from about 13% copolymer concentration all the way up to the melt. Curiously, the exponent is in close agreement with the incompressible field theory approach[16,18] generalized to solutions based on phenomenological blob scaling arguments.[15,21] However, such agreement seems fortuitous since the scaling arguments apply only in semidilute solution, while all the data (except perhaps for the lowest concentration sample) are in concentrated solution for which the phenomenological theories predict the dilution approximation should hold! Moreover, the polyolefin sample also follows a scaling law, but with an apparent exponent in between the dilution approximation and semidilute scaling values.[19] Thus, it appears that an unidentified, nonuniversal process is controlling the relation between the critical value of N and copolymer concentration. However, as we shall demonstrate below, the nonuniversal influence of solvent dilution on the local interchain packing of copolymers, which is accounted for by PRISM theory, modifies the effective χ parameter (which is ultimately determined by microscopic scale interactions) in a manner consistent with the experiments cited above.

It is worth pointing out that such a "puzzle" of scaling theory working well outside its regime of validity is also present to some extent in polystyrene (PS) homopolymer solutions.[22] Here, the semidilute scaling laws relating the polymer density screening length (or mesh size), ξ_ρ, and concentration persist up to the highest measured polymer concentrations of $\approx$ 30−40% volume fraction. This is well beyond the semidilute regime; for example, for a 40% PS solution in good solvent, $\xi_\rho \simeq 6$ Å corresponding to a "mesh size" equal to a monomer diameter! Clearly under such conditions scaling arguments are not valid since they require low, semidilute polymer densities and the inequality $\xi_\rho \gg d, \sigma$, where d and σ are the monomer diameter and statistical segment length, respectively. Similar comments appear to apply to the osmotic pressure as a function of polymer concentration.[23] Finally, an additional complication is that the polymer volume fraction dependence of chain dimensions in homopolymer good (semidilute and concentrated) solutions, and the accuracy of semidilute scaling laws (e.g., $R_g \propto \phi^{-1/8}$), remains poorly established experimentally.[17,24] Such difficulties in homopolymer solutions further complicate the theoretical analysis of copolymer solutions.

Microdomain scale concentration fluctuation effects could also, in principle, play a role in the failure of the dilution approximation. However, prior arguments based on the BLFH theory[16,18] and our own PRISM studies suggest such effects enter in a minor, secondary manner. Nevertheless, other experimental measurements,[20] such as the intensity of small angle scattering and visual microscopy, are sensitive to long-range fluctuations, the character of which is modified in solution relative to the melt behavior. Such experiments motivate our application of PRISM theory to compute how various equilibrium properties are influenced by microdomain scale concentration fluctuations in solution. Of special interest is the fascinating microscopy observation by Lodge and co-workers[20] of segregated patterns, or "fluctuating microstructure", in semidilute solutions of compositionally asymmetric diblock copolymers even very far from the ODT. We believe this is a consequence of the strongly enhanced physical clustering tendency of copolymers in the more (osmotic) compressible solution state. PRISM calculations of structural properties which support this idea will be presented.

The remainder of the paper is structured as follows. Both the phenomenological blob scaling and microscopic PRISM theory of homopolymer solutions are briefly summarized in section II. These results are crucial input into the copolymer solution analysis. Scaling and field theoretic predictions for copolymer solutions are briefly reviewed in section III. Section IV introduces our simple Gaussian thread model of copolymer solutions and the general statistical mechanical aspects of PRISM theory. Limiting analytic results and connections with blob scaling and field theory approaches are also discussed. Model calculations based on experimentally realistic parameters are presented in section V. The relative importance of local versus microdomain scale concentration fluctuations is established for structural and thermodynamic quantities. Comparison with recent measurements is made, and the influence of nonuniversal local features such as nonzero chain thickness and semiflexibility are explored based on numerical PRISM computations. The paper concludes in section VI with a summary and discussion. For the sake of saving space, we assume the reader is familiar with refs 9 and 12 and quote the results derived there which are required for our present work.

II. Theories of Homopolymer Solutions

Fundamental structural and thermodynamic properties of homopolymer solutions[4,25,26] include the polymer density screening length or "mesh size", ξ_ρ, single chain end-to-end distance, R, and the osmotic pressure, Π, which are all dependent on polymer volume fraction, ϕ. Modern scaling[4,26] and renormalization group (RG)[26−28] ideas have been developed which predict the large N qualitative form of the universal (power law) dependence of these properties on polymer concentration in the good and Θ solvent semidilute regime $\phi^* \ll \phi \ll \phi^{**}$, where $\phi^* \propto N/R^3$. However, the crossover from semidilute to the concentrated regime at $\phi = \phi^{**}$ (believed to be at $\phi^{**} \approx 0.2-0.3$), and the corresponding nonpower law dependence of these properties on ϕ, are not predicted by scaling approaches and are expected to be sensitive to system-specific nonuniversal features. In principle, the microscopic PRISM theory approach[11] can

treat all polymer concentration regimes. In this section we summarize and contrast scaling theory and PRISM predictions for homopolymer solutions, which are required as a starting point to treat copolymer solutions.

A. Blob Scaling Approach. The key idea in semidilute solution[4,25,29] is that the fundamental length scale is the N-independent mesh size, ξ_ρ, and polymer−polymer interactions influence properties only via a reduced concentration, ϕ/ϕ^*. This physically-motivated scaling ansatz, plus knowledge of the dilute solution scaling relation between chain size and degree of polymerization, $R \propto N^\nu$, leads immediately to the scaling prediction

$$\xi_\rho \propto \phi^{-\nu/(3\nu-1)}\sigma_0 \qquad \phi^* \ll \phi \ll \phi^{**} \tag{1}$$

where σ_0 is an N- and concentration-independent fundamental length. In good solvents the RG (Flory mean field) value of ν is 0.588 (3/5), while $\nu = {}^1/_2$ in ideal solvents, thereby implying $\xi_\rho \propto \phi^{-0.77}$ ($\phi^{-3/4}$) or ϕ^{-1}, respectively. The blob concept[4] corresponds to the idea that for length scales smaller than the mesh size a polymer chain behaves as if it were in dilute solution, but for distances larger than the mesh size, ideal random walk statistics applies. A single chain is viewed as an ideal random coil composed of "blobs" of size ξ_ρ. The number of blobs, N_b, is related to the true number of segments, N, by the relation[4] $N_b(\phi) = N/g$, where $g \cong \phi(\xi_\rho/\sigma_0)^3$ is the number of segments per blob. The chain dimensions in semidilute solution is given by[4]

$$R^2(\phi) \cong N_b\xi_\rho^2 \propto N\phi^{-(2\nu-1)/(3\nu-1)}{\sigma_0}^2 \tag{2}$$

The good solvent behavior is $R \propto \phi^{-0.115}$($\phi^{-1/8}$). The solution structure is viewed as a dense-packed "melt" of noninterpenetrating blobs. The osmotic pressure follows from a simple ideal gas like law:

$$\Pi \cong k_B T/{\xi_\rho}^3 \propto {\sigma_0}^{-3}\phi^{3\nu/(3\nu-1)} \qquad \phi^* \ll \phi \ll \phi^{**} \tag{3}$$

The derivation of eqs 2 and 3 do *not* require use of the blob concept.[25] Thus, even within the phenomenological scaling framework, blobs are a theoretical construct of secondary importance.

In the high density concentrated regime the intrachain excluded volume interactions are "screened", and the blob concept and scaling theory are not valid.[4,25] This regime has been traditionally described by a self-consistent, Edwards mean field type approach.[25,30] However, since it is based on the idealized Edwards Hamiltonian[31] and polymers of infinitesimal thickness, this approach is not expected to be adequate under highly concentrated or melt conditions.

Equations 1 and 3 have been extensively tested experimentally, especially for polystyrene solutions,[22,23,29] and the predicted scaling laws appear to be remarkably accurate under both good and Θ solvent conditions. However, as emphasized by Brown,[22] a mystery is that the scaling laws "work too well" in the sense that they apply for situations where the assumptions of the scaling approach are not valid. For example, the mesh size obeys the semidilute scaling law up to concentrated solutions of $\phi = 0.3$ (good) and 0.4 (Θ). Under these highly concentrated conditions, for polystyrene solutions $\xi_\rho \cong 6$ Å (good solvents) and 12 Å (Θ solvents) which are comparable to all the nonuniversal microscopic length scales in the system such as the chain persistence length and monomer diameter. Due to experimental difficulties,[22] there appear to be virtually no data for more concentrated solutions which connect the scaling laws with the melt behavior. However, it is clear that power law scaling must break down, and the osmotic pressure (screening length) increases (decreases) more and more rapidly as the nearly incompressible melt state is approached in a manner which is not expected to be universal.[11,25] Thus, the screening length in a polystyrene melt should be less than the solution extrapolation[22] of roughly 3 Å.

Equation 2 has not been thoroughly tested. The few direct measurements on polystyrene good solutions do not agree.[24] It is unclear if the predicted exponent in semidilute good solution is accurate, nor has the crossover to an ideal ϕ-independent chain dimension been unambiguously established.

Since our theoretical approach for the copolymer problem is based on liquid state theory, we now discuss its predictions for homopolymer semidilute solutions. The question of how the concentrated and melt state is treated within the same conceptual framework is also addressed.

B. PRISM Theory. We consider the simplest possible model of homopolymer solutions. The solvent is treated as a continuum or vacuum; the polymer is treated as a Gaussian chain with an effective statistical segment length $\sigma(\phi)$, a *fixed* number of segments N, and a vanishing thickness ("thread").[11,32] This model is very similar to that adopted in continuum field theories.[25,31] However, the "blob" idealization is *not* invoked. Rather, microscopic interactions are accounted for via the hard core constraint that the intermolecular site−site pair correlation (radial distribution) function vanishes at contact; i.e., $g(r = 0) = 0$. For good or "athermal" solvent conditions this completes the specification of the "thread model".

PRISM theory with the Percus−Yevick (PY) closure[11,33] is employed to calculate the interchain site-site packing correlations, $g_0(r)$, and collective polymer density fluctuation structure factor in Fourier space $S(k) = \omega(k) + \rho h_0(k)$. Here, the subscript "0" denotes the athermal solution situation, ρ is the polymer segment number density which can be expressed as $\rho = \phi\rho_m$ where ρ_m is the corresponding melt value, $h_0(r) = g_0(r) - 1$, and $\omega(k)$ is the single polymer structure factor which is approximated by the following simple Lorentzian form:[25] $\omega(k) = 1/[(k^2\sigma^2/12) + N^{-1}]$. In principle, the intrachain and interchain pair correlations can be self-consistently solved for within the framework of PRISM theory.[11,34−36] However, here we adopt the simpler approach of assuming the single chain correlations are known. In the context of the effective Gaussian model, this corresponds to an a priori specification of the effective segment length $\sigma(\phi)$. For semidilute solutions we employ the following scaling prediction: $\sigma(\phi) = \sigma_0\phi^{-(2\nu-1)/[2(3\nu-1)]}$.

Analytical solution of the PRISM-PY integral equation theory yields[11,32]

$$g_0(r) = 1 + \frac{3}{\pi\rho\sigma^2 r}[e^{-r/\xi_\rho} - e^{-r/\xi_c}] \tag{4}$$

$$S(k) = \frac{12\sigma^{-2}}{k^2 + {\xi_\rho}^{-2}} \tag{5}$$

$$S(0) = 12(\xi_\rho/\sigma)^2 \tag{6}$$

where the polymer density screening is given by

$$\xi_\rho^{-1} = \frac{\pi}{3\rho\sigma^2} + \sqrt{\frac{12}{N}}\sigma^{-1} \tag{7}$$

For large N above the semidilute crossover, eq 7 has the classic invariant form, $\xi_\rho \propto (\rho\sigma^2)^{-1}$. The interchain pair correlation function is always less than unity and consists of three terms: the leading naive mean field value of unity, a spatially local nonuniversal contribution due to polymer density correlations characterized by the mesh length scale ξ_ρ, and a long range "correlation hole" contribution due to the universal consequences of chain connectivity and uncrossability characterized by the length scale $\xi_c = (N/12)^{1/2}\sigma = R_g/\sqrt{2}$.

As discussed previously, the above results for the screening length and $S(k)$ are in remarkable agreement with phenomenological blob scaling and field theoretic (with three body repulsive interactions[31]) predictions for semidilute solutions.[11,32] Similar agreement applies for the osmotic pressure, given by $\beta\Pi = \int_0^\rho d\rho' S^{-1}(0;\rho')$, the second and third virial coefficients, and the semidilute crossover concentration.[25,32,36] When an attractive site−site tail potential is added, Θ solvents and thermal effects can be explicitly addressed, including the polymer−solvent demixing transition, its critical properties, and the Θ temperature.[37] The thread model cannot be *quantitatively* accurate in concentrated and melt conditions due to its neglect of the nonzero thickness and semiflexibility of real polymer chains. An analytic generalization of the thread model, known as the "string model",[11,32,37,38] approximately takes the nonzero segment hard core diameter into account. Recent work[37] has shown this simple model can provide a very good description of the rapid, non power law growth (reduction) of the osmotic pressure (screening length) in concentrated solutions up to the melt state. This analysis suggests the semidilute scaling laws remain accurate up to 30−40% polymer volume fraction.

In subsequent sections, we shall employ two simple models to describe the screening length over the entire semidilute−concentrated melt regimes which incorporate available experimental and theoretical knowledge for solutions and the melt state. These models are graphically illustrated in Figure 1. In both models one must first decide what is the melt density screening length, which is expressed in dimensionless form as the system-specific parameter $(\xi_\rho/\sigma_0)_{melt}$. For polystyrene, and other typical flexible polymers, $\sigma_0 \cong 5 - 7$ Å. If one uses eq 7 and known melt properties,[39] or if one extrapolates the polystyrene solution measurements of the mesh size in Θ and good solvents,[22] then the estimate $\xi_\rho \cong 2 - 6$ Å is obtained corresponding to $(\xi_\rho/\sigma_0)_{melt} \cong 0.3 - 1$. On the other hand, on the basis of eq 6 and the known typical density and isothermal compressibility of polymer melts, one obtains[40,41] the estimate $(\xi_\rho/\sigma_0)_{melt} \cong 0.14-0.25$.

On the basis of a reasonable choice for the dimensionless melt parameter, the polymer concentration dependence is determined in two distinct manners. For "model 1", we assume the semidilute laws hold all the way up to the melt and thus set $\xi_\rho/\sigma = (\xi_\rho/\sigma_0)_{melt}\phi^{-\delta}$, where $\delta = 1$ (θ) and $^5/_8$ (good). For "model 2", we use the experimental data for the screening length of polystyrene solutions:[22] $\xi_\rho = 2.7\phi^{-0.72}$ Å ($6.3\phi^{-1}$ Å) for good (Θ) solvents up to $\phi = 0.4$ and $\sigma_0 = 6$ Å. For the $0.4 < \phi < 1$ concentrated solution regime, the chain dimensions are assumed to be independent of ϕ (ideal statistics), and ξ_ρ/σ_0 is obtained by smoothly interpolating between the experimental semidilute value at $\phi = 0.4$ and the (chosen) melt value.

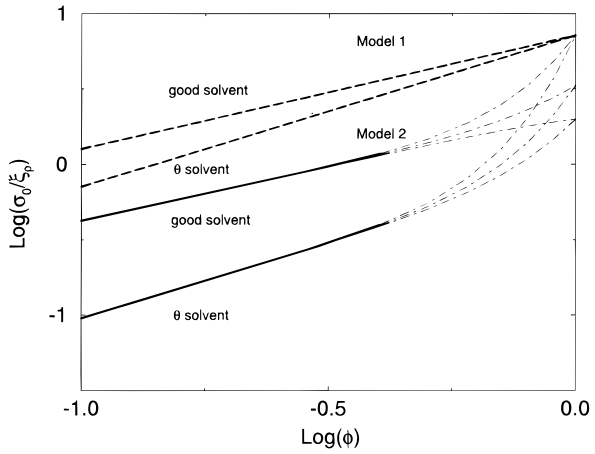

Figure 1. Model calculations for the inverse normalized density screening length σ_0/ξ_ρ in solution (semidilute-concentrated-melt regimes) as a function of the polymer volume fraction ϕ. The chosen parameters correspond to a polystyrene sample with a melt statistical segment length of $\sigma_0 \approx 6$ Å. In model 1 (long dashed curve), the semidilute scaling laws are assumed for all concentrations. In model 2 (solid curves), the experimental semidilute scaling behavior for polystyrene ($\xi_\rho = 2.7\phi^{-0.72}$ Å in good solvent and $\xi_\rho = 6.3\phi^{-1}$ Å in Θ solvent) is employed and smoothly interpolated (long−short dashed curves) to the various chosen melt values of $(\xi_\rho/a)_{melt} = 0.28$, 0.6, 1, where $a = \sigma_0/2$.

Examples of these models for the screening length are shown in Figure 1. We believe the variability seen there is representative of the range of possibilities in homopolymer solutions. Our copolymer solution predictions for the concentration dependence of the effective χ parameter are sensitive to the (nonuniversal) magnitude and concentration dependence of ξ_ρ/σ in the concentrated and melt regime. Direct measurements, or a truly quantitative theory, are required to make an unambiguous choice of ξ_ρ/σ for a specific polymer−solvent mixture. Numerical PRISM calculations for a more chemically realistic chain model are presented in section VB to further address this issue.

III. Scaling and Field Theories of Copolymer Solutions

Fredrickson and Leibler[16] and de la Cruz[18] have independently generalized both the mean field and the fluctuation-corrected BLFH theories to treat semidilute AB diblock copolymer solutions. The generalization is based on blob scaling arguments, renormalization group results for the analogous AB semidilute blend problem,[15] and overall mixture incompressibility ("pseudo-binary" approximation). The solvent is assumed to be neutral, and complete structural and interaction symmetry between the A and B species is adopted. The latter simplification corresponds to the idealized "symmetric model".

At the mean field Leibler theory level, the net effect of dilution is 2-fold: replacement of the number of segments by the number of blobs $N \rightarrow N/g(\phi)$, and renormalization of the blob−blob AB effective χ parameter due to reduction of the number of pair contacts in good solvents, i.e. $\chi_{mf} \rightarrow \chi_{mf}\phi^\lambda$, where $\lambda \cong 0.29$ and χ_{mf} is the classical mean field χ parameter (defined here to be polymer concentration independent). With these substitutions, the mean field spinodal condition (which

is usually very close to the mean field ODT condition[16]) in semidilute good solvents is given by[16,18]

$$(\chi_{mf}N)_{ODT}\phi^{1.61} = F(f) \tag{8}$$

or at fixed temperature

$$\phi_{ODT} \propto N^{-0.62} \tag{9}$$

where $F(f)$ is well-known[5] [≅10.5 for symmetric (and nearly so) diblock compositions] and is equal to the critical value $\chi_s N$ corresponding to a mean field spinodal divergence at the unstable wave vector $k^* \propto R_g^{-1}$. The RG value for ν has also been employed. Equation 8 can be equivalently interpreted as the mean field Leibler expression but with an effective χ-parameter which is proportional to $\phi^{1.61}$. In the concentrated solution regime ($\phi > \phi^{**}$) the dilution approximation is predicted[16,18] to be recovered corresponding to the exponent replacement of 1.61 → 1. Recent experiments clearly disagree with this prediction.[19]

de la Cruz[18] has discussed the generalization to semidilute Θ solvents, based on the blob scaling theory of blend solutions of Onuki and Hashimoto.[21] Although Θ conditions may be very hard to achieve in practice, this case is of considerable theoretical interest. For the strongly incompatible A and B blocks of primary relevance, the results are[18]

$$(\chi_{mf}N)_{ODT}\phi^{2} = F(f) \tag{10}$$

$$\phi_{ODT} \propto N^{-1/2} \tag{11}$$

corresponding to even stronger deviations from the dilution approximation than for good solvents. In concentrated solutions, the dilution approximation is again predicted to be recovered.

Incorporation of fluctuation effects in good solvents within the BLFH approach follows the same procedure as described above.[16,18] The bare χ parameter is renormalized by the excluded volume interaction, and N is replaced by the number of blobs. Within the BLFH framework, fluctuation effects have been argued[16,19] to make only a small correction to eqs 8 and 9 and not to be the source of strong deviations from the dilution approximation. One additional, possibly testable, prediction is that the peak scattering intensity at the ODT is given by[16,18]

$$\left[\frac{S(k^*)}{N}\right]_{ODT} \propto N_b(\phi)^{1/3} \propto \phi^{\lambda}N^{1/3} \tag{12}$$

where $\lambda = {}^5/_{12}$ (good solvent; $\nu = {}^3/_5$) or ${}^2/_3$ (Θ solvent), and our normalization of $S(k^*)$ has divided out a factor of ϕ relative to the experimental total intensity.

IV. PRISM Theory of Copolymer Solutions

A. Model and Closure Approximations. We consider the simplest "symmetric" Gaussian thread model of AB copolymer solutions which is essentially equivalent to that adopted by the field theory plus scaling approaches. The difference is we employ the compressible PRISM theory of diblock solutions as discussed in Section IIB. The linear diblock chain is composed of fN A segments and $(1 - f)N$ B segments which interact via identical site−site hard core repulsions. Structurally, the A and B blocks are considered identical in every respect except there is an AB repulsive tail potential, $v_{AB}(r)$, which mimics the enthalpic incompatibility associated with a positive χ parameter. This quite simple model captures the essential physics of the problem and allows analytical results to be derived. A screened Coulomb form is employed for analytic convenience

$$v_{AB}(r) = \epsilon\frac{e^{-r/a}}{r/a} \tag{13}$$

where $\epsilon > 0$ and "a" is the spatial range parameter which is expected to by an intrinsic, ϕ-independent property. For this model, in the high temperature athermal limit the system reduces to a *homopolymer solution* for *all* copolymer compositions, f.

The three coupled PRISM equations for AA, BB, and AB correlations and their approximate solution based on molecular closures in the thread limit have been discussed in depth elsewhere.[9] For the symmetric model, PRISM theory predicts a concentration fluctuation structure factor, $S_\phi(k)$, of the same form as the incompressible RPA expression[4], but with a renormalized effective χ parameter. On the basis of the most sophisticated linearized "Reference Molecular Percus Yevick" (R-MPY) closure approximation, one obtains[9,11]

$$\chi = \rho_m\phi\int d\mathbf{r}\, \beta v_{AB}(r)g_{AB}(r) \tag{14}$$

where $g_{AB}(r)$ is the intermolecular site−site pair correlation functions between A and B segments on different copolymers. This function includes both local concentration (or "polymer density") fluctuations, which are present even in the high temperature "athermal" limit (as discussed in Section IIB), and a contribution associated with microdomain scale concentration fluctuations. The latter couples to the local AB packing in a finite size manner, and leads to a self-consistent link between the effective chi-parameter and $S_\phi(k)$ on the k^* scale.[9] Physically, as the diblock fluid is cooled, A and B segments tend to avoid each other in order to lower the system free energy and thereby reduce χ. This local nonrandom mixing process influences microdomain scale fluctuations due to chain connectivity and destroys all spinodal and critical divergences. An analogous fluctuation process occurs in blends but serves only to renormalize the effective χ parameter and not destroy the macroscopic phase separation transition.[42] This level of PRISM is roughly the liquid state theory analog of the BLFH theory,[12] although the underlying physical mechanism of fluctuation stabilization is very different and involves coupled monomer (total density) and composition fluctuations.[9]

Equation 14 can be simplified by neglecting certain correlation effects. These simplifications correspond to different closure approximations for the species-dependent site−site direct correlation functions.[9] A "high temperature approximation" (HTA), or "thermodynamic perturbative" approach, corresponds to replacing the full thermal $g_{AB}(r)$ by its athermal analog. This simplification is called the R-MPY/HTA closure approximation. For the symmetric model one obtains

$$\chi = \rho_m\phi\int d\mathbf{r}\, \beta v_{AB}(r)g_0(r) \equiv \chi_{hta} \tag{15}$$

where $g_0(r)$ is given by eq 5. Equation 15 retains the influence of local *athermal* interchain pair correlations on the effective χ parameter which serve to reduce the effective χ parameter in a *concentration and system-*

specific manner. However, the χ parameter is now "deterministic". That is, since the effect of microdomain scale concentration fluctuations and physical clustering on the effective χ parameter are neglected, spinodal divergences are recovered.[9] This level of PRISM might be viewed as the analog of Leibler theory[5] generalized to copolymer solutions. However, there are differences since PRISM treats the packing of chains in a microscopic fashion as opposed to using the phenomenological blob scaling ansatz.

The crudest approximation is to adopt the Flory-like assumption of complete random mixing, i.e. $g_{AB}(r) = 1$. Equation 14 then reduces to the off-lattice analog of the Flory χ parameter

$$\chi = \rho_m \phi \int d\mathbf{r}\, \beta v_{AB}(r) = 4\pi\beta\epsilon\rho_m a^3 \phi \equiv \chi_0 \qquad (16)$$

where the last equality defines the mean field "bare" χ parameter ($\chi_0 = \phi\chi_{mf}$ in our notation). Hence, PRISM theory for the symmetric thread model reduces to Leibler theory for $S_\phi(k)$, and the dilution approximation is recovered. This crudest level of PRISM follows from the so-called R-MMSA molecular closure approximation.[11]

B. Local Concentration Fluctuations. Substituting eq 4 into eq 15 and using eq 16 yield for large N

$$\frac{\chi_{hta}}{\chi_0} = \frac{1}{1 + (\xi_\rho/a)} \qquad (17)$$

The effective χ parameter is reduced due to the *local* correlation hole, which is an entropic packing effect. For the idealized symmetric model, this ratio is f-independent. The magnitude of the effect depends on both the intrinsic spatial range of the tail potential ($a \cong \sigma_0/2$ for Lennard-Jones type interactions[32] is adopted here) and the concentration- and materials-specific polymer density screening length. The corresponding spinodal divergence condition is given by

$$(\chi_{hta}N)_s = F(f) \equiv \chi_s N \qquad (18)$$

and hence

$$\left[\frac{4\pi\beta\epsilon\rho_m a^3 \phi N}{1 + 2(\xi_\rho/\sigma_0)}\right]_s = F(f) \qquad (19)$$

The polymer concentration dependence of the microphase separation spinodal temperature $T_{hta,s}$ at fixed N, or critical value of N_s at fixed temperature, is not given by the dilution approximation and depends sensitively on the magnitude and concentration dependence of the mesh size. There are three general types of behavior.

In a high density or hypothetical incompressible polymer subsystem limit, one has $\xi_\rho/a \ll 1$ and the dilution approximation is recovered whence $\phi_s \propto N^{-1}$. However, on the basis of the discussion in section II, we do not believe this limit is achievable over any significant range of ϕ since melt screening lengths are expected to be no smaller than roughly 1 Å.

In the semidilute solution regime, $\xi_\rho/a \gg 1$, which results in a significant reduction of AB contacts due to local excluded volume packing effects. Using eq 1 in eqs 18 and 19 yields

$$\phi_{ODT} \propto N^{-(3\nu-1)/(4\nu-1)} \qquad (20)$$

$$T_{ODT} \propto N\phi^{(4\nu-1)/(3\nu-1)} \qquad (21)$$

where the known near identity of the spinodal and ODT condition at the mean field level[5] has been employed. Remarkably, these predictions exactly agree with the blob scaling field theory results for both good and Θ solvents.[16,18]

In the concentrated regime of relevance to recent experiments, the ratio ξ_ρ/a is of order unity. In this crossover situation, system-specific apparent scaling exponents may emerge, or non power law behavior could occur. This case is numerically studied in section V.

C. Microdomain Scale Concentration Fluctuations and Physical Clustering. As discussed in detail previously,[9,12] using the PRISM equations and a dominant one wave vector approximation, eq 15 can be manipulated into a single nonlinear cubic equation for either the effective χ parameter or the square root of the peak scattering amplitude $S^{1/2}(k^*;T,N,f,\xi_\rho/a)$. Here we focus on the theoretical predictions for copolymer solutions. The dimensionless or normalized form of the self-consistent PRISM/R-MPY theory cubic equation is given by[12]

$$(t/\sqrt{N_{eff}})s(k^*)^{1/2}(s(k^*) - 1) + (1 - t)s(k^*) - 1 = 0 \qquad (22)$$

$$N_{eff} = \frac{\bar{N}}{[\Theta'(1 + \xi_\rho/a)]^2} \qquad (23)$$

where $s(k^*) = S(k^*;T)/S(k^*;\, T = \infty)$, $t = T_{hta,s}/T$, $\bar{N} = N(\rho_m\phi\sigma^3)^2$, $\Theta' = x^*/\{\alpha f(1 - f)[2F(f)]^{1/2}\}$, $x^* = (k^*R_g)^2$, α is a known numerical constant of order unity (e.g., $\alpha = 1.102$ for $f = {}^1/_2$), and $T_{hta,s}$ follows from eq 19. Note that all the explicit dependence on polymer concentration enters via an effective degree of polymerization N_{eff}. In melt BLFH theory[6], the identical concentration-dependent quantity $\bar{N}$ enters and entirely controls the fluctuation effects, while for the semidilute good solvent case the fluctuation correction enters via the replacement $N \rightarrow N_{blob} = N/g(\phi) \cong N/[\phi(\xi_\rho/\sigma_0)^3]$. In contrast, the corresponding replacement in PRISM theory is $N \rightarrow N(\xi_\rho/a)^{-2}$. Curiously, for semidilute Θ solvents the concentration dependence of these two replacements agree that $N \rightarrow N\phi^2$, but for good solvents there is a small difference: $N \rightarrow N\phi^{3/2}$ (PRISM) and $N \rightarrow N\phi^{5/4}$ (BLFH). In the concentrated regime the ϕ-dependence of the fluctuation correction of PRISM and BLFH agree only if $\xi_\rho/a \ll 1$, a limit not very probable for real compressible fluids. For both theories, the amplitude of the fluctuation effects and the breadth of the non mean field regime are predicted to be enhanced as the copolymer melt is diluted with a nonselective solvent. However, as discussed in the next section, the microdomain scale concentration fluctuation correction to the order−disorder phase transition condition is sufficiently modest that it is of secondary importance relative to the corrections which arise at the HTA (mean field like) level discussed in the previous subsection.

PRISM is a liquid state theory and hence does not predict a true microphase separation transition to a long-range ordered state. An empirical prescription based on the disordered phase scattering intensity to estimate an "apparent" ODT has been recently suggested:[12] T_{ODT} is defined as the linear extrapolation of the $S^{-1}(k^*)$ vs T^{-1} curve at the extrapolated spinodal (or "mean field") temperature $T_{hta,s}$. The idea is sketched in Figure 2, and the explicit result is

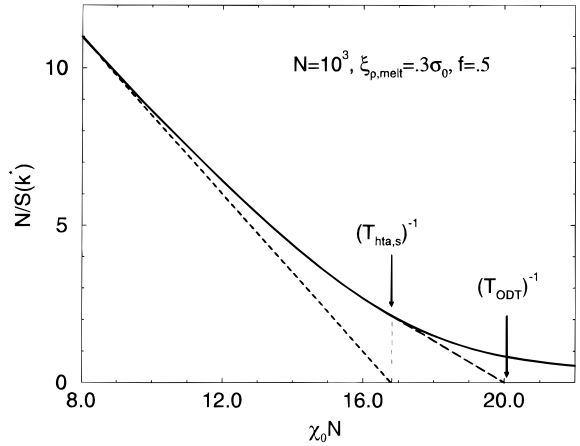

Figure 2. Example calculation demonstrating how the "apparent" order−disorder transition temperature (T_{ODT}) is determined[12] from the inverse normalized static structure factor as a function of $\chi_0 \propto T^{-1}$. The shown result is computed with PRISM-RMPY theory, for a symmetric ($f = {}^1/_2$) diblock copolymer ($N = 1000$, $\xi_{\rho,melt} = 0.3\sigma_0$). The extrapolated HTA spinodal temperature ($T_{hta,s}$) is also shown.

$$T_{ODT} = T_{hta,s}\left\{1 + \frac{3}{2}\left(\frac{1}{2\chi_s N}\right)^{1/3}\left[\frac{x^*(1+\xi_\rho/a)}{\alpha f(1-f)}\right]^{2/3}\bar{N}^{-1/3}\right\}^{-1} \quad (24)$$

This empirical approach to computing T_{ODT} provides surprisingly good predictions when applied to both experimental data and the BLFH theory.[12] The temperature shift $\Delta T = T_{hta,s} - T_{ODT} \propto N^{-1/3}$, and for large N one obtains $S(k^*) \propto N^{4/3}$ at both $T_{hta,s}$ and T_{ODT}, in qualitative agreement with BLFH theory.[6]

Equations 22−24 are self-consistently solved numerically to obtain the critical degree of polymerization required for the copolymer solution to microphase separate at a given copolymer concentration and fixed temperature. Model calculations are presented in the next section.

The peak scattering intensity at the apparent ODT has been analytically determined for large N to be[9]

$$\left[\frac{S(k^*)}{N}\right]_{ODT} = \left[\frac{\alpha f(1-f)}{2F(f)x^*(1+\xi_\rho/a)}\right]^{2/3}\bar{N}^{1/3} \quad (25)$$

In semidilute solution, one obtains (using $\nu = {}^3/_5$ in good solvent)

$$[S(k^*)/N]_{ODT} \propto (\phi\sigma^3)^{2/3}(a/\xi_\rho)^{2/3}N^{1/3} \propto \phi^{[1+2\nu]/[3(3\nu-1)]}N^{1/3} \propto \phi^{11/12}\ (good) \quad (26)$$

$$\propto \phi^{4/3}\ (\Theta) \quad (27)$$

which correspond to concentration scaling exponents roughly twice as large as the blob scaling results of eq 12. The origin of this difference appears to be the use of N, and not $\bar{N}$, in the copolymer solution field theories.[16,18] This distinction was not made in the original version of BLFH theory[6] due to the implicit assumption of a close-packed lattice-like model when the incompressibility constraint was enforced. If N is replaced by $\bar{N}$ in the fluctuation correction part, then essentially complete agreement between eq 12 and PRISM theory is obtained.[12]

A measure of real space local physical clustering is given by the following differences in *contact* values of the interchain pair correlation functions[42,43]

$$\Delta g_{AA} = g_{AA} - g_{AB} = f^{-1}\Delta G \qquad \Delta g_{BB} = g_{BB} - g_{AB} = (1-f)^{-1}\Delta G \quad (28)$$

$$\Delta G = [3/(\pi\rho\sigma^3)](6/N)^{1/2}\{(a\tilde{s})^{1/2} - (b\tilde{s})^{-1/2} - [a/2F(f)]^{1/2} + [b/2F(f)]^{-1/2}\} \quad (29)$$

where $\tilde{s} = S(k^*)/N$, $a = 3/[2f^2(1-f)^2]$ and $b = 1/[2f(1-f)]$. The above equations apply above the semidilute crossover concentration, where the leading factor of ΔG is proportional to the length scale ratio ξ_ρ/R_g, which controls the strength of the finite size coupling of microdomain and local correlations. In the athermal limit, ΔG vanishes as it must.

If $f = {}^1/_2$, then by symmetry $\Delta g_{AA} = \Delta g_{BB} = \Delta g$. For compositionally asymmetric copolymers, significantly larger physical clustering occurs for the minority species than the majority block, and clustering is enhanced as N is decreased and/or the system is cooled. In a cooling experiment, three regimes of behavior are predicted. The first is high temperature far from the ODT where $\Delta g \propto N^{-1/2}\ \phi^{-1/[2(3\nu-1)]} \propto \phi^{-1}$ (Θ solvent) $\phi^{-5/8}$ (good solvent). The second is the ODT. For large N in semidilute solution $\Delta g \propto N^{-1/3}\ \phi^{-1}\sigma^{-3}(\sigma/\xi_\rho^2)^{1/3} \propto N^{-1/3}\phi^{(\nu-1)/[3(3\nu-1)]} \propto \phi^{-1/3}$ (Θ solvent) or $\phi^{-1/6}$ (good solvent). The third is the low temperature supercooled liquid regime $T \ll T_{ODT}$. In semidilute solutions PRISM predicts $S(k^*)/N \propto N[\rho_m\phi\sigma^3(a/\xi_\rho)]^2$ which implies $\Delta g \propto N^0\phi^{2\nu/[2(3\nu-1)]} \propto \phi^1$ (Θ solvents) and $\phi^{3/4}$ (good solvents). Note that even at a fixed thermodynamic state the ϕ dependence of the local clustering function, Δg, is predicted to be significantly different in Θ and good solvents, being stronger under ideal Θ conditions. Moreover, the effect of solvent dilution is subtle. Many chain clustering is enhanced by solvent dilution far from, and at, the ODT, which can be interpreted as due to the enhanced copolymer osmotic compressibility upon dilution which facilitates the fluctuation process. However, local clustering is reduced by dilution at low temperatures well below the ODT, where nearly pure microdomains are present.

As previously pointed out, PRISM theory below the ODT crudely describes the system as a highly correlated, but globally isotropic, fluid. For simplicity, possible stretching of the polymer chains has been ignored in this paper. However, prior PRISM analysis and numerical mean field theory studies[44] suggest coil stretching is not significant even below the ODT until a strong segregation regime is entered, where $\chi N \geq 100$. The BLFH theory is also not expected to be accurate far below the ODT. Thus, our results in the latter regime are less reliable and perhaps only of qualitative value.

At, and below, the ODT the ϕ dependence of local clustering in concentrated solutions (up to the melt) will depend on the detailed magnitude and concentration dependence of the screening length or mesh size. Numerical examples will be given in section V.

The BLFH predictions for Δg at high temperature and at the ODT in semidilute solutions are quite similar to the PRISM results since the corresponding behavior of $S(k^*)/N$ is similar. However, the low-temperature PRISM predictions are very different from the corresponding BLFH results. This is because BLFH theory predicts at low temperature that $S(k^*)/N \propto N(N/T)^2$, which is in strong contrast with the PRISM prediction of saturation of the peak scattering intensity.[6,9] The latter behavior is required in order that the physically sensible strong segregation result of $\Delta g \propto N^0$ is obtained.

Finally, for other experimental protocols the response of local clustering to a change in the control parameter can be particularly subtle even at, or above, the ODT. We shall be concerned with two distinct situations. (i) If temperature and copolymer concentration are fixed and the ODT is appoached by increasing N, then there are two opposite effects: increasing N reduces the strength of the finite size fluctuation process which tends to decrease Δg, but Δg is enhanced by the fact that the ODT is approached as N is increased and $S(k^*)/N$ grows. (ii) If T and N are fixed and the ODT is approached by increasing copolymer concentration, there are again two competing effects: increased ϕ reduces the osmotic compressibility, which suppresses local clustering, but Δg is enhanced since the ODT is approached as ϕ is increased and $S(k^*)/N$ grows. Numerical examples of such competitions are given in section VC.

V. Model Calculations and Experimental Comparisons

In this section we present numerical applications of the PRISM theory described in sections II and IV. We have chosen values for system parameters to mimic the experimental situation. Our primary goal is to establish the range of predicted behaviors and possible trends. Comparisons with experiment will be semiquantitatively discussed, which we believe is the appropriate level given the limited experimental data, nonuniversal parameter uncertainties, and the relatively crude nature of the Gaussian thread analytic PRISM theory.

A. Fluctuation Effects on ODT Concentration Scaling. Here we are interested in determining the predictions of PRISM theory for the connection at the ODT between copolymer volume fraction and degree of polymerization *under constant temperature conditions* of relevance to recent experiments. We choose as the constant temperature the *melt* ODT temperature, $T = T_{ODT}(N_{melt};\ \phi = 1)$, for various choices of $N = N_{melt}$. Equations 18, 19, and 24 are employed to predict the value of N at the ODT of a copolymer solution of concentration ϕ *at the temperature* T. Values of N_{melt} are considered which span the range relevant to recent experiments: $N_{melt} = 200-2000$. Three different values of the reduced melt screening length are considered which span the experimental range as estimated in section II: $(\xi_\rho/\sigma_0)_{melt} = 0.14$, 0.3, and 0.5. To describe the ϕ dependence of the mesh size in good and Θ solutions, we employ the two procedures discussed in section IIB: "model 1" based on a smooth extrapolation of the melt value to solutions under the assumption that the semidilute scaling laws apply for all polymer concentrations, and "model 2" based on experimental data for polystyrene solutions, the assumption of chain ideality above $\phi = 0.4$, and a smooth interpolation up to the (chosen) melt screening length.

Selected results for good and Θ solvents, several choices of N_{melt} and screening length model, at the HTA theory level and also with long range concentration fluctuation corrections, are plotted in Figures 3 and 4 in a log−log format. Results are given for solutions in the range $0.1 < \phi < 1$ corresponding to the end of the semidilute regime and the full concentrated regime up to the melt. Power law fits are shown in the figures and the effective exponents δ, defined as $\phi_{ODT} \propto N^{-\delta}$, are listed in Tables 1 and 2. In all cases, rather remarkable agreement with an apparent power law behavior is found. There are systematic deviations from a power law, but we suspect their magnitude is smaller than the inherent uncertainties in most (or all) existing experimental measurements.

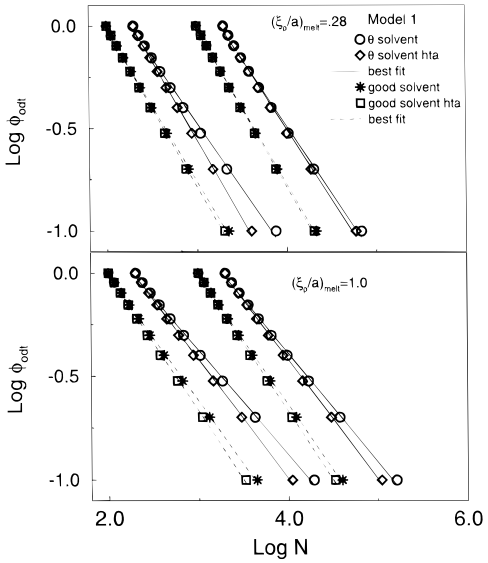

Figure 3. PRISM model calculations of the polymer volume fraction at the ODT as a function of degree of polymerization, in good and Θ solvents (the data for Θ solvents are shifted by log 2 to avoid superposition). Results with and without (hta) the concentration fluctuation contribution are shown based on screening length model 1. The temperature is fixed at the melt ODT transition temperature for $N = 200$ or $N = 1000$. Results for two values of the density screening length, $(\xi_\rho/a)_{melt} = 0.28$ and 1, are shown. The best fit power law curves correspond to the apparent scaling exponents reported in Table 1.

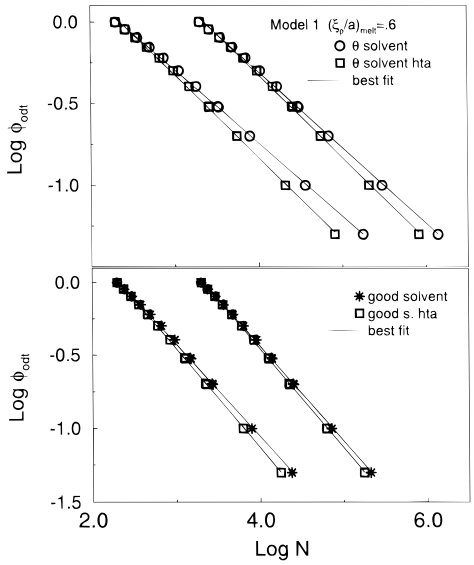

Figure 4. PRISM model calculations of the polymer volume fraction at the ODT as a function of degree of polymerization, in good and Θ solvents. Results with and without (hta) the concentration fluctuation contribution are shown based on screening length model 2. The temperature is fixed at the melt ODT transition temperature for $N = 200$ or $N = 2000$. Results for one value of the density screening length, $(\xi_\rho/a)_{melt} = 0.60$, are shown. The best fit power law curves correspond to the apparent scaling exponents reported in Table 2.

There are many systematic trends evident in our calculations. Consider first the results based on model 1 (Table 1 and Figure 3). (1) Strong deviations from the dilution approximation are always found, although there is generally a weakening of this deviation if only the highly concentrated regime is analyzed ($0.5 < \phi < 1$). (2) The inclusion of long-range concentration fluc-

Table 1. Model 1 Based Apparent Scaling Exponents of Polymer Volume Fraction at the ODT as a Function of Degree of Polymerization ($\phi_{ODT} \propto N^{-\delta}$) for Several Choices of Melt $N = 200$, 1000, and 2000 and $(\xi_\rho/a)_{melt} = 0.28$, 0.6, and 1[a]

$(\xi_\rho/a)_{melt}$		$N = 200$	$N = 1000$	$N = 2000$	HTA
0.28	$0.1 < \phi < 1$	0.74 (0.64)	0.75 (0.65)	0.76 (0.66)	0.77 (0.68)
	$0.5 < \phi < 1$	0.82 (0.75)	0.82 (0.76)	0.83 (0.77)	0.84 (0.79)
0.60	$0.1 < \phi < 1$	0.66 (0.55)	0.67 (0.57)	0.67 (0.57)	0.70 (0.61)
	$0.5 < \phi < 1$	0.725 (0.64)	0.73 (0.66)	0.74 (0.67)	0.76 (0.70)
1.0	$0.1 < \phi < 1$	0.61 (0.51)	0.62 (0.52)	0.63 (0.53)	0.66 (0.58)
	$0.5 < \phi < 1$	0.66 (0.58)	0.67 (0.59)	0.68 (0.60)	0.71 (0.64)

[a] Best-fit exponents for good solvents from semidilute concentration to the melt ($0.1 \leq \phi \leq 1$) are shown in the first line, and the exponents from a best fit of only the concentrated regime ($0.5 < \phi < 1$) are shown on the second line. The large N limiting HTA result is also shown. The corresponding best fit exponents in Θ solvents are given in parentheses.

Table 2. Model 2 Based Apparent Scaling Exponents of Polymer Volume Fraction at the ODT as a Function of Degree of Polymerization ($\phi_{ODT} \propto N^{-\delta}$) for Several Choices of Melt $N = 200$, 1000, and 2000 and $(\xi_\rho/a)_{melt} = 0.28$, 0.6, and 1[a]

$(\xi_\rho/a)_{melt}$	solvent	$N = 200$	$N = 1000$	$N = 2000$	HTA
0.28	$0.1 < \phi < 1$	0.61 (0.41)	0.62 (0.42)	0.63 (0.42)	0.64 (0.44)
	$0.5 < \phi < 1$	0.50 (0.33)	0.51 (0.33)	0.51 (0.33)	0.53 (0.34)
0.60	$0.1 < \phi < 1$	0.63 (0.43)	0.64 (0.44)	0.65 (0.44)	0.67 (0.48)
	$0.5 < \phi < 1$	0.57 (0.35)	0.585 (0.36)	0.59 (0.36)	0.62 (0.38)
1.0	$0.1 < \phi < 1$	0.65 (0.43)	0.66 (0.44)	0.67 (0.45)	0.705 (0.50)
	$0.5 < \phi < 1$	0.68 (0.39)	0.70 (0.40)	0.71 (0.40)	0.76 (0.43)

[a] Best fit exponents for good solvents from semidilute concentration to the melt ($0.1 \leq \phi \leq 1$) are shown in first line, and the exponents from a best fit to only the concentrated regime ($0.5 < \phi < 1$) are shown on the second line. The large N limiting HTA result is also shown. The corresponding best fit exponents in Θ solvents are given in parentheses.

tuations always reduces the effective exponents computed at the "mean field" (HTA) level since fluctuations preferentially stabilize the lower concentration solutions. However, this exponent reduction is a rather small, secondary effect, which diminishes with increasing N (and approaches the HTA theory value as $N \rightarrow \infty$) since fluctuation stabilization is a finite size effect. (3) Deviations from the dilution approximation increase as the melt screening length increases and/or the solvent quality changes from good to Θ. Again, this is simply because the naive Flory mean field approximation of $g(r) = 1$ worsens if these changes are made. (4) For parameters we believe are most relevant to the PS−PI good solvent case ($N_{melt} = 200$, $(\xi_\rho/a)_{melt} = 0.6 - 1.0$), an effective exponent (over the entire ϕ range) of 0.61−0.66 is found, in agreement with the experimental value[19] of roughly 0.63. The corresponding Θ solvent value is predicted to fall in the range 0.51−0.55, which again is accidentally close to the semidilute scaling exponent of $^1/_2$.

We emphasize that a unique, unambiguous mapping of real chemical systems onto the parameters of our symmetric Gaussian thread copolymer model is not really possible. Thus, our primary conclusion is that the PRISM theory predictions are consistent with the very strong deviations from the dilution approximation seen experimentally in good solvents, and also its nonuniversality and/or dependence on the ϕ-regime analyzed. The primary physical origin is very simple: dilution reduces local interchain contacts/packing between copolymer segments which results in a ϕ-dependent reduction of the effective enthalpic χ parameter. In addition, the agreement of the concentrated good solution PS−PI data with the semidilute blob scaling arguments is clearly fortuitous within the framework of our theory.

Consider now the results in Figure 4 and Table 2 based on model 2 for the mesh size. For most cases, the concentration dependence of the screening length above a copolymer volume fraction of 0.4 is considerably stronger than that for model 1. As a consequence, the effective exponents are generally smaller; i.e., they deviate even more from the dilution approximation value of unity, and the apparent exponents in the highly concentrated regime are usually *smaller* than those over the full concentration range. These differences are quite small in good solvents, but considerably larger in Θ solvents. For example, exponents as small as 0.35−0.4 appear to be possible in concentrated solution, values even farther removed from the dilution approximation than the semidilute scaling prediction of 0.5. Nevertheless, all other trends found for model 2 remain qualitatively the same as for model 1. For the PS−PI good solvent type parameters discussed above ($N_{melt} = 200$, $(\xi_\rho/a)_{melt} = 0.6-1.0$), an effective exponent (over the entire ϕ range) of 0.61−0.65 is predicted for *all* choices of melt mesh size, in excellent agreement with the experimental observation and in accidental agreement with the semidilute scaling exponent.

B. Influence of Chain Thickness and Semiflexibility. The analysis of the above section suggests the primary origin of the failure of the dilution approximation is the modification of local interchain packing by solvent addition. Although the Gaussian thread model provides a reasonable description of this physical process, it is expected to be an oversimplification, particularly at high concentrations. To investigate the influence of local chemical features such as semiflexibility and nonzero backbone thickness (d) on interchain packing, we employ the "semiflexible chain model" (SFC)[36] and numerical PRISM theory. The parameters of the SFC model are selected as described previously to accurately reproduce both the conformational and interchain packing of polymers in the melt.[40] The relevant values of chain aspect ratios $\Gamma = \sigma/d$ are 0.8−1.4 for a wide range of polymer melts. The melt reduced density is selected to be $\rho_m d^3 = 1.375$ in order to reproduce the experimental melt dimensionless compressibility of $S(0) = 0.25$ at 430 K for polyethylene ($\Gamma = 1.2$).[40] Solutions are modeled as one-component fluids of reduced site density of $\phi\rho_m d^3$. Good and Θ solvent conditions are described following the idea of model 1; i.e. for Θ solvents the aspect ratio is independent of concentration, but for good solvents $\Gamma(\phi) = \Gamma_{melt}\phi^{-1/8}$. In contrast with the thread model, the polymer mesh length does not have to be estimated from external information; instead, it is automatically predicted by PRISM theory for all polymer concentrations. Experi-

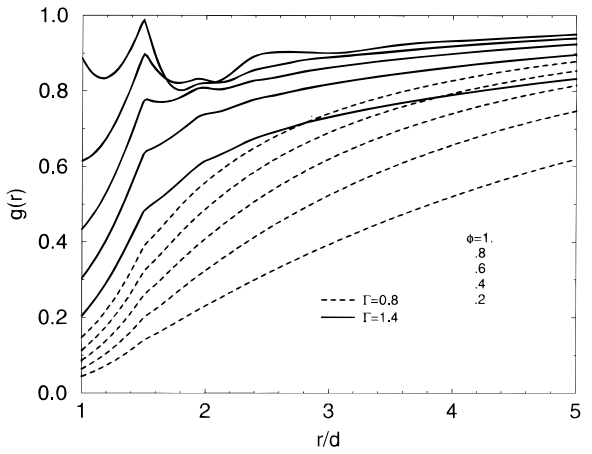

Figure 5. PRISM site−site intermolecular pair correlation functions vs the normalized intersite distance (r/d) for the semiflexible chain model and the two extreme melt aspect ratios studied, $\Gamma = 0.8$, 1.4. Results are shown for increasing polymer volume fraction ($\phi = 0.2$, 0.4, 0.6, 0.8, 1) under model good solvent conditions.

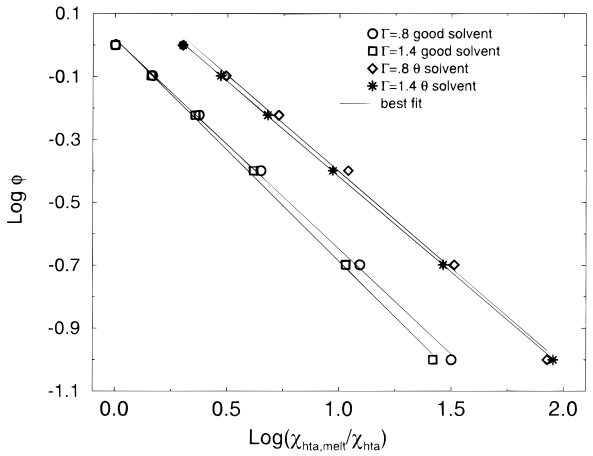

Figure 6. PRISM semiflexible chain model calculations of the polymer volume fraction at the ODT as a function of the normalized HTA chi parameter. Results in good and Θ solvents for the two extreme melt aspect ratios are shown. The temperature is fixed at the melt ODT transition temperature for a polymer with $N = 1000$ and the corresponding stiffness. The Θ solvent results are shifted by a factor log 2 for clarity.

mentally reasonable behavior is expected due to the established accuracy of athermal homopolymer PRISM[11] and the fact that we have "calibrated" the reduced site density to reproduce the correct melt value of isothermal compressibility and hence the density fluctuation amplitude.[40]

A value of $N = 1000$ is employed which yields a local structure representative of high polymers. A purely hard core intersite pair interaction is adopted for the calculation of structure consistent with the HTA approach. The numerical procedures to compute the required pair correlation functions and solve the PRISM equation are described elsewhere.[36,40] To treat thermal copolymer solutions (based on the symmetric copolymer model), we employ a shifted repulsive Lennard−Jones tail potential $v_{AB}(r)$ between A and B sites on different chains.[40,41] This is the more realistic analog of the Yukawa form of eq 13. Since at the HTA theory level, N and inverse temperature are interchangeable in the spinodal condition (see eq 18), we report our graphical results in the form of ϕ plotted vs a normalized inverse χ parameter $\chi_{hta}(\phi = 1)/\chi_{hta}(\phi)$ in a log−log format. This ratio quantifies the deviation from the dilution approximation and is equal to the factor $[1 + (\xi_\rho(\phi)/a)]/\{\phi[1 + (\xi_\rho/a)_{melt}]\}$ in the thread model.

Selected athermal interchain $g(r)$'s are shown in Figure 5 for a range of solution concentrations and the two extreme melt aspect ratios considered. Reduction of polymer density and/or aspect ratio reduces local interchain contacts.[11,40] A strong dependence of $g(r)$ on polymer concentration on the local length scale of the intermolecular tail potential is predicted, which never goes away even in concentrated solution. These trends are in qualitative accord with the thread model predictions. Also note that the absolute magnitude of $g(r)$ on local scales is very sensitive to the chain aspect ratio. However, the relative change with polymer concentration is quite similar for all values of Γ_{melt}.

Examples of the normalized inverse χ parameter as a function of ϕ are shown in Figure 6. Good power law fits are obtained. The corresponding effective exponents δ, defined as $\phi_{ODT} \propto N^{-\delta}$, are given in Table 3 for several model systems. The dependence of the effective exponents on chain aspect ratio is quite weak. For both solvent quality models the apparent exponents fall in the rather narrow range of 0.63 ± 0.06, consistent with the PS−PI good solvent data.[19] In accord with the thread results, the apparent exponents are smaller for Θ solvents compared with their good solvent analog. The high concentration regime apparent exponents are generally slightly smaller than that extracted from a fit to all the calculations. We note that the effective exponents in Table 3 span a rather narrow range compared with the results of Tables 1 and 2.

Table 3. Apparent Scaling Exponents $\phi_{ODT} \propto N^{-\delta}$, Based on the Numerical PRISM/HTA Theory Using the Semiflexible Chain Model[a]

	$\Gamma = 0.8$	$\Gamma = 1$	$\Gamma = 1.2$	$\Gamma = 1.4$
good solv	0.67	0.66	0.68	0.70
Θ solv	0.61	0.57	0.57	0.61
good solv $1 \le \phi \le 0.5$	0.60	0.58	0.60	0.62
Θ solv, $1 \le \phi \le 0.5$	0.52	0.50	0.54	0.585

[a] Best fit values for good and Θ solutions of polymer models of variable aspect ratio, Γ, are listed based on the semidilute to melt range ($0.1 \le \phi \le 1$), and in the concentrated regime ($0.5 \le \phi \le 1$).

Summarizing, we find it significant and encouraging that PRISM/HTA level numerical calculations based on a chemically realistic model of a symmetric copolymer are in good accord with the corresponding analytic predictions based on the highly simplified Gaussian thread model. Similar agreement between numerical and analytic PRISM calculations has been previously documented for several physical problems[11] such as melt solubility parameters[40] and the miscibility of conformationally and interaction asymmetric blends[10,41] and diblock copolymer melts.[9,10,35]

C. Peak Scattering Intensity and Physical Clustering. Although long-range concentration fluctuations only weakly influence the effective ODT scaling exponents, they do have other striking consequences on equilibrium properties which are amenable to experimental study. In addition, within the microscopic mode-coupling theory of entangled chain dynamics,[45] both microdomain scale fluctuations and local real space clustering play an important role in generating additional frictional resistance to entangled copolymer motion.[43] In this section we present model calculations based on eqs 22, 23, 24, and 28 in a format relevant to experiments. Our goal is to establish the general nature

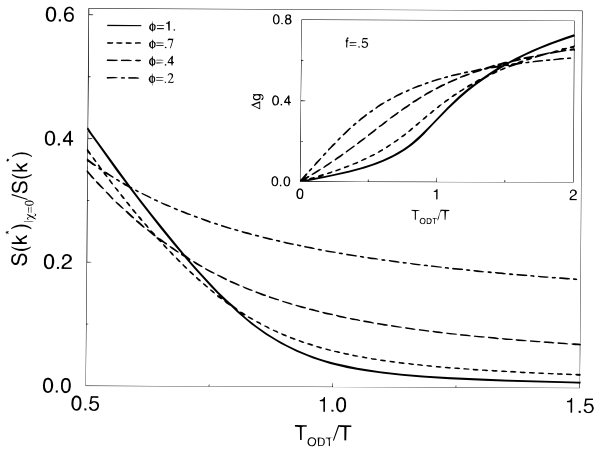

Figure 7. Normalized inverse peak scattering intensity for a $N = 1000$ symmetric diblock copolymer solution as a function of the normalized inverse temperature, under model good solvent conditions at variable polymer volume fraction ϕ, based on screening length model 2 with $(\xi_\rho/\sigma)_{melt} = 0.3$. The inset shows the corresponding interchain clustering pair correlation function at contact.

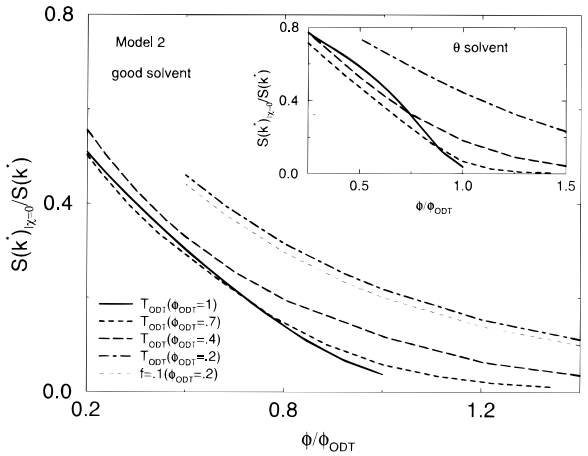

Figure 8. Normalized inverse peak scattering intensity at fixed temperature $[T_{ODT}(\phi_{ODT})]$ for a $N = 1000$ symmetric block copolymer solution as a function of the polymer volume fraction (ϕ) under good solvent conditions based on screening length model 2 with $(\xi_\rho/\sigma)_{melt} = 0.3$. The ODT is approached by increasing the polymer concentration, and results for $\phi_{ODT} = 0.2$, 0.4, 0.7, and 1 are shown. Changing the block copolymer composition has very little effect (see light dashed curve for $f = 0.1$). In the inset we report the corresponding plot for Θ solvent conditions.

of the PRISM predictions. Unless indicated otherwise, all calculations are for $N = 1000$, $f = 1/2$, screening length model 2, $(\xi_\rho/\sigma_0)_{melt} = 0.3$, and good solvents.

The inverse peak scattering intensity versus inverse temperature is plotted in Figure 7 in a normalized fashion for several copolymer concentrations. The basic trend is increased disordered phase stabilization (suppression of $S(k^*)$) at fixed thermodynamic state (T_{ODT}/T value) as the copolymer concentration is reduced. This trend is a consequence primarily of increased copolymer osmotic compressibility which enhances the enthalpically-driven fluctuation feedback mechanism.[9] Qualitatively similar results are found for Θ solvents (not shown), but the sensitivity to concentration is more pronounced due to the larger and more ϕ-dependent nature of ξ_ρ.

The inset to Figure 7 shows the corresponding real space physical clustering function at contact. There are several trends. (a) Clustering is monotonically enhanced with cooling, and tends to saturate at low temperatures. (b) Quantitatively significant values are found near the ODT even for the rather large degree of polymerization considered. (c) Above, and near, the ODT the clustering strongly increases as the copolymer concentration is reduced, and the onset occurs at higher reduced temperature. (d) Below the apparent ODT (supercooled fluctuating phase)[9,12] there are "curve crossings" where the trends are reversed. All the behaviors (a−d) are in qualitative accord with the analytic results discussed in section IVC.

Normalized inverse peak scattering intensity predictions are shown in Figure 8 for the case where the temperature is fixed at $T_{ODT}(\phi_{ODT})$ for several choices of ϕ_{ODT}, and the ODT is approached by increasing copolymer concentration. Again, there is a tendency for larger suppression of microdomain scale fluctuations as the copolymer volume fraction is reduced, in both good and Θ (see inset) solvents. Physically, this is due to the increased finite size coupling of microdomain and local concentration fluctuations in solutions of enhanced osmotic compressibility. Although not shown, the detailed behavior for theta solvents is particularly sensitive to the screening length model (1 or 2) and the value of $(\xi_\rho/\sigma_0)_{melt}$ chosen.

The light short-dashed curve in the main part of Figure 8 is for a $\phi_{ODT} = 0.2$ solution of a compositionally

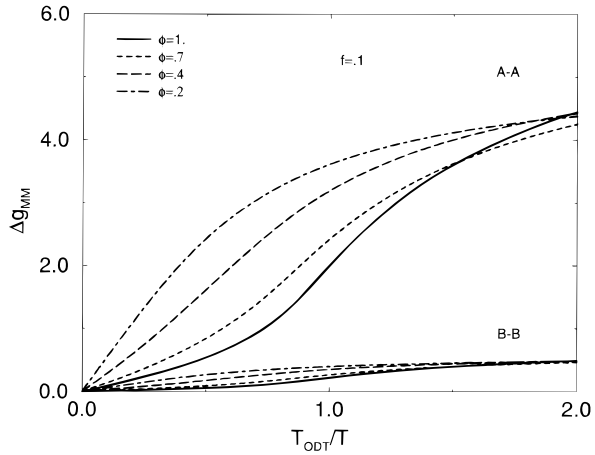

Figure 9. Species-dependent contact interchain clustering pair correlation function as a function of the normalized inverse temperature for a $N = 1000$ highly asymmetric ($f = 0.1$) block copolymer good solvent solution. Results for several polymer volume fractions, ϕ, are shown based on model 2 with $(\xi_\rho/\sigma)_{melt} = 0.3$. The minority species ($A$) shows a greatly enhanced physical clustering with respect to the majority species (B).

asymmetric copolymer of $f = 1/10$. As discussed previously,[9,12] when examined in a reduced variable format PRISM theory predicts a near independence of the inverse peak scattering intensity on f, a behavior in strong contrast with the BLFH theory.[6] On the other hand, the temperature-dependent physical clustering in this compositionally asymmetric case is dramatically larger for the minority species compared to the majority species (see Figure 9). The shape of the Δg_{MM} curves are very similar to the symmetric $f = 1/2$ case (see inset of Figure 7 and eq 28). However, near the ODT the amplitude of the clustering is roughly an *order of magnitude greater* for the minority $f = 0.1$ species than for the $f = 0.5$ symmetric system. A consequence is that a melt-like ODT value of minority species clustering is attained in 20% solution *very far* from its ODT, i.e. at roughly $T \cong 0.25T_{ODT}$. Such dramatically enhanced physical clustering in solutions of highly compositionally asymmetric diblocks of modest degree of polymerization

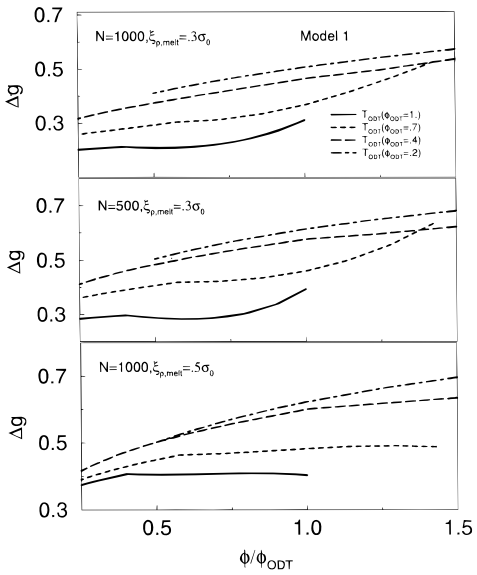

Figure 10. Contact interchain clustering pair correlation function at fixed temperature $[T_{ODT}(\phi_{ODT})]$ for a symmetric block copolymer solution as a function of the polymer volume fraction (ϕ), in good solvent model 2 for four choices of ϕ_{ODT}. The curves are modified in a modest manner by changing the polymer degree of polymerization and/or the melt density screening length.

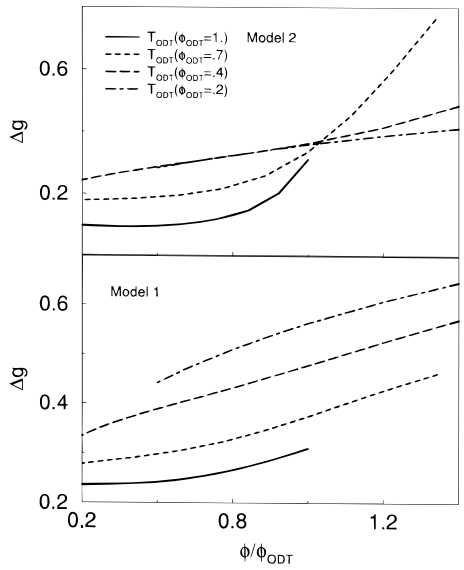

Figure 11. Contact interchain clustering pair correlation function in Θ solvent solution at fixed temperature $[T_{ODT}(\phi_{ODT})]$ for a $N = 1000$ symmetric block copolymer as a function of the polymer volume fraction (ϕ), and $(\xi_\rho/\sigma)_{melt} = 0.3$. The ODT is approached by increasing the polymer concentration. Screening length model 1 (lower curve) results in more gentle trends than model 2 (upper curve).

even very far away from the ODT has been recently observed via transmission electron microscopy by Lodge and co-workers[20] for PS−PI solutions in neutral solvents. Of course, the visual observation of (fluctuating) microdomain patterns and a large Δg are not precisely equivalent phenomena, but the latter is physically required if the former occurs.

Figure 10 shows examples of the N and melt screening length dependence of the local clustering at $T = T_{ODT}(\phi_{ODT})$ as a function of reduced copolymer concentration for the fixed $f = {}^1/_2$, good solvent case, and several choices of ϕ_{ODT}. The molecular weight dependence of the clustering follows the trends predicted analytically in section IVC: roughly $N^{-1/2}$-dependent far from the ODT, which weakens at the ODT, and almost N-independent far below the ODT. There is a remarkably gentle dependence on distance from the ODT as measured by ϕ/ϕ_{ODT}, and a relatively weak dependence of the clustering amplitude on ϕ_{ODT}. These trends are due to the near compensation of the two competing effects associated with increasing concentration as discussed at the end of section IVC.

Close to the melt state a stronger dependence on concentration emerges, although the precise behavior is sensitive to the (nonuniversal) magnitude of the melt screening length and its concentration dependence (e.g. model 1 vs model 2). This sensitivity is even more evident under Θ conditions as shown in Figure 11. Much smoother curves are obtained based on "model 1" (lower panel) than based on "model 2". Nevertheless, both screening length models do predict qualitatively similar behaviors.

VI. Summary and Discussion

The present, and prior, theoretical work has demonstrated that there is a rather remarkable agreement *in semidilute solution* between the predictions of the phenomenological blob scaling approach for homopolymers, and also (at the mean field level) blends and block copolymers, with the corresponding analytic predictions of the simplest version of PRISM theory[9−11,32,36,37] based on a hard core Gaussian thread model, a simple Yukawa tail potential, and a HTA-like molecular closure approximation. We believe this agreement is significant for two reasons. First, it demonstrates that an approximate microscopic compressible liquid state theory formulated at the level of segments and interchain potentials can recover nonclassical scaling results. Second, it provides a theoretical rationale for why the scaling predictions often work in regimes where the assumptions employed in their derivation do not apply. That is, the blob scaling predictions emerge from PRISM theory as a consequence of chain connectivity and intermolecular forces even when the density fluctuation screening length is not vast compared to local chemical length scales.

In contrast, the blob scaling approaches have nothing to say about the concentrated regime where the screening length is of order or much less than the statistical segment length. Simple Flory-like mean field behavior is predicted (the dilution approximation), which follows essentially from the (incorrect) assumption of local interchain random mixing. In contrast, since PRISM is a microscopic theory, it naturally can account for local nonrandom packing in concentrated and melt states due to interchain repulsions. This physical process is concentration-dependent in a qualitatively obvious manner and is predicted to be the dominant one leading to the failure of the dilution approximation observed experimentally in concentrated copolymer solutions. Moreover, model calculations based on physically realistic parameters do predict apparent power law behavior. The effective exponents fall in a range that agrees with recent experiments,[19] and for some cases fortuitous agreement with the semidilute scaling laws is found. Equally importantly, the theory predicts strong nonuniversality of the effective exponent depending on solvent quality and chemical structure. Although we cannot rule out other explanations or physical mechanisms for the failure of the dilution approximation, no other mechanism appears to be required to account for the existing experimental data.

PRISM theory is in qualitative accord with the BLFH plus blob scaling analysis[16,18] conclusion that the influence of finite size microdomain scale fluctuation effects on the effective scaling exponent, and failure of the dilution approximation question, is weak.[16,19] However, future experiments in near Θ neutral solvents with very low molecular weight diblocks (e.g. $N = 25-50$ in the melt) may reveal significant changes in the apparent scaling exponents.

We have also established via asymptotic analytic analysis and model calculations the systematic trends predicted by PRISM theory for fluctuation effects on microdomain scale scattering intensity and local physical clustering. Qualitatively, our predictions are quite similar to the BLFH plus blob scaling theory[16,18] for compositionally *symmetric* diblock solutions, although strong deviations occur for compositionally asymmetric cases.[12] The latter cases are particularly interesting since PRISM theory predicts the scattering intensity behavior will be very similar to $f = {}^1/_2$ systems when examined in a reduced variable format,[9,12] *but* extremely strong physical clustering of the minority species occurs even far from the ODT. This prediction is in qualitative accord with recent microscopy experiments.[20]

With regards to future experiments and/or simulations to further test our theory, we have several obvious suggestions.

(a) Rational manipulation of the magnitude of the melt screening length (via chemical modification) or attainment of (near) Θ conditions can result in significant changes in effective scaling exponents. Isotopic diblocks would be the ideal system to employ. Alternatively, judicious selection of A and B monomers and solvent could result in a system with nearly equivalent (by accident) homopolymer solution Θ temperatures.

(b) Our HTA level theory predictions directly apply to the related AB blend solution problem. For this system, the predictions of PRISM theory at the same symmetric model and statistical mechanical levels considered in this paper have been thoroughly worked out both analytically and numerically.[11,42] Virtually identical predictions for the solution concentration dependence of the effective χ parameter of blends and diblocks are found. This is easy to understand since at the HTA level local packing correlations in the reference athermal solution are the origin of deviations from the dilution approximation, and this effect is identical for long chain blends and block copolymers. The blend PRISM theory has been qualitatively compared[42] with Monte Carlo simulations of Binder and co-workers.[46] Excellent agreement is found for all the non-Flory–Huggins(FH) effects observed in the simulations except, of course, the Ising critical exponent aspect. In particular, PRISM theory and the simulations find very strong deviations from the dilution approximation, sometimes reported as the renormalized critical temperature $T_C/T_{C,FH}$, which is less than unity and decreases significantly with polymer dilution. Long-range concentration fluctuation effects are also predicted and are observed in simulation to be much smaller in blends than for diblocks. However, there are observable consequences such as a nearly parabolic blend composition-dependence of the effective χ parameter. PRISM theory with the linearized R-MPY closure has been shown to be in excellent accord with such thermodynamic and structural consequences of long-range concentration fluctuations seen in the blend simulations (again, except for the Ising exponent).[42] Future simulation/theory comparisons should focus on a quantitative comparison of the blend solution dependence of the critical temperature on polymer concentration. In addition, experiments on the same chemical system in the blend and diblock states would be very valuable to test the general idea that deviations from the dilution approximation are primarily of local packing origin. Isotopic blends and diblocks would be the ideal systems to employ.

(c) The HTA level theory predictions also directly apply to the related AB multiblock copolymer solution. However, long-range concentration fluctuation effects may be much more important here, especially for blocky copolymers where the microdomain ordering and local length scales are much closer. PRISM theory including fluctuation effects has been recently worked out for multiblocks.[47]

(d) Many new measurements of $S(k^*)$ as a function of T, f, N, ϕ, and solvent quality are required to test our predictions for fluctuation stabilization in solution. As a general comment, more direct experimental data for chain dimensions and screening length, in both the homopolymer and copolymer states, as a function of solution concentration would be of great value as input to the theory. Mayes et al.[17] have recently done some work in this direction. Computer simulation[48] may also be of value since modest chain lengths may be adequate for addressing the above questions.

It is worth considering the limitations of the present work, additional complications when making comparisons with experiment, and future theoretical extensions. We have ignored possible chain stretching near the ODT. This effect has been included within PRISM theory but results in a small correction.[35] We do not believe it can generate a correction to the dilution approximation which is significant relative to the other sources of non-mean-field behavior considered in this paper. If one wants to understand the subtle ϕ dependence of k^* or R_g, as recently probed by Mayes et al.,[17] then inclusion of chain stretching may be crucial.

The influence of local chemical structure beyond a Gaussian type model and the molecularity of the solvent may be significant for some systems. These aspects can be addressed using established numerical PRISM methods and chemically realistic models, and this generalization is presently being pursued for homopolymer solutions.[37]

The "structurally and interaction symmetric" model employed in this paper is inadequate for predicting the *absolute magnitude* of chi-parameters and phase transition temperatures, and for establishing *chemical and conformational correlations* of such properties.[10] This problem has been thoroughly addressed analytically using Gaussian thread PRISM theory, a Bertholet model for the interchain attractive tail potentials, and the RMPY-HTA closure.[10] In the long-chain limit, the form of the spinodal temperature for an AB diblock (or blend with $f \rightarrow$ A-monomer volume fraction) is given qualitatively by[10]

$$T_s \propto \left[\frac{\epsilon_A \rho_m \phi a^3}{1 + \xi_{\rho,\mathrm{eff}}/a}\right] \frac{Nf(1-f)(\gamma^2-\lambda)^2}{f + \gamma^4(1-f)} \qquad (30)$$

$$\xi_{\rho,\mathrm{eff}} \propto (\phi \rho_m \sigma_A{}^2)^{-1}[f + \gamma^2(1-f)]^{-1} \qquad (31)$$

where $\gamma = \sigma_B/\sigma_A$ quantifies the "structural or conformational asymmetry", λ^2 is the ratio of the bare dispersion interaction energy strengths for A and B segments and quantifies the "interaction or chemical" asymmetry, and

"a" is again the spatial range of the (Yukawa) attractive dispersion potential. The solution concentration dependence of the leading factor in brackets of eq 30 is the same as found in the present paper based on the "structurally symmetric" model, *except* the copolymer inverse density screening length is a composition-dependent average of the corresponding homopolymer solution values. The simple interpolative form of the screening length seems physically sensible. The ϕ-dependent screening length has the same concentration dependence as the corresponding homopolymer solutions, although its ϕ-dependent magnitude will introduce changes in our predictions for the effective scaling exponent and other properties. The above features of the effective screening length are in good agreement with the recent neutron scattering measurements of Mayes et al.[17] on homopolymer and diblock copolymer solutions of polystyrene and polymethylmethacrylate.

There is, however, another complication.[10,35] The A and B block statistical segment lengths, and hence the conformational asymmetry parameter γ, are (in general) expected to depend not only on solution concentration ϕ, but also on copolymer (or blend) composition f. This question of nonideal corrections to single chain dimensions in structurally asymmetric polymer alloys is poorly understood, but clearly could significantly influence the theoretical predictions in a nonuniversal manner. The fully self-consistent version of PRISM theory[34,35] could be employed to address this question. Such a program has been successfully carried out for homopolymer (good) solutions[34] and "symmetric" models of AB blends[49] and diblock copolymers.[35] Generalization to treat the more interesting conformationally and interaction asymmetric case beyond the prior qualitative discussion level[35] remains to be done.

Finally, recent experiments on AB blend and block copolymer melts subjected to modest external pressure have revealed a complex, nonuniversal behavior.[50] Pressure can enhance or reduce long wavelength concentration fluctuations and miscibility depending on the specific system. Present theoretical understanding is quite poor due to the subtlety of the phenomena deriving from the multiple property changes induced by pressure. These include modifications of A and B chain dimensions, fluctuation stabilization process, total density, compressibility contributions to the free energy, local packing, etc. For example, the full form of eq 30 contains a positive contribution of the order N^0 which is proportional to the copolymer melt isothermal compressibility. This contribution is expected to *decrease* with applied pressure. On the other hand, the factor in brackets of the leading of order N^1 term *increases* with density(pressure), *but* the conformational asymmetry contributions may increase, decrease, or not change depending on the system. Thus, PRISM theory has the potential to include many competing effects, but specific predictions may often be sensitive to material-specific input parameters.

Acknowledgment. This work was supported by the Department of Energy via UIUC-MRL Grant No. *DEFG*02-91*ER*45439 and Sandia National Laboratory CRADA #1087. We thank Dr. Ted David for use of computer programs, helpful discussions, and contributions to the early stage of this project. We also thank Professor Tim Lodge for sending preprints, tables of data, and helpful discussions. M.G. is a member of the permanent staff of IMAG-CNR and thanks the National Research Council of Italy for the opportunity to carry out this research at the University of Illinois at Urbana-Champaign.

References and Notes

(1) Bates, F. S.; Fredrickson, G. H. *Annu. Rev. Phys. Chem.* **1990**, *41*, 525.
(2) Binney, J. J.; Dowrick, N. J.; Fisher, A. J.; Newman, M. E. J. *The Theory of Critical Phenomena*; Oxford Science Publications: Oxford, G. B., 1992.
(3) Flory, P. J. *Statistical Mechanics of Chain Molecules*; Cornell University Press: Ithaca, NY, 1953.
(4) de Gennes, P. G. *Scaling Concepts in Polymer Physics*; Cornell University Press: Ithaca, NY, 1978.
(5) Leibler, L. *Macromolecules* **1980**, *13*, 1602.
(6) Fredrickson, G. H.; Helfand, E. *J. Chem. Phys.* **1987**, *87*, 697.
(7) Brazovskii, S. A. *Sov. Phys. JETP* **1975**, *41*, 85.
(8) Stepanow, S. *Macromolecules* **1995**, *28*, 8233.
(9) David, E. F.; Schweizer, K. S. *J. Chem. Phys.* **1994**, *100*, 7767, 7784.
(10) Schweizer, K. S. *Macromolecules* **1993**, *26*, 6033, 6050.
(11) Schweizer, K. S.; Curro, J. G. *Adv. Chem. Phys.* **1997**, *98*, 1. Schweizer, K. S.; Curro, J. G. *Adv. Polym. Sci.* **1994**, *116*, 319 and references cited therein.
(12) Guenza, M.; Schweizer, K. S. *J. Chem. Phys.* **1997**, *106*, 7391.
(13) Helfand, E.; Tagami, Y. *J. Chem. Phys.* **1972**, *56*, 3592.
(14) Hong, K. M.; Noolandi, J. *Macromolecules* **1983**, *16*, 1083. Whitmore, M. D.; Noolandi, J. *J. Chem. Phys.* **1990**, *93*, 2946.
(15) Joanny, J.-F.; Leibler, L.; Ball, R. *J. Chem. Phys.* **1984**, *81*, 4640. Broseta, D.; Leibler, L.; Joanny, J.-F. *Macromolecules* **1987**, *20*, 1935.
(16) Fredrickson, G. H.; Leibler, L. *Macromolecules* **1989**, *22*, 1238.
(17) Mayes, A. M.; Barker, J. G.; Russel, T. P. *J. Chem. Phys.* **1994**, *101*, 5213.
(18) Olvera de la Cruz, M. *J. Chem. Phys.* **1989**, *90*, 1995.
(19) Lodge, T. P.; Pan, C.; Jin, X.; Liu, Z.; Zhao, J.; Maurer, W. W.; Bates, F. S. *J. Polym. Sci., Polym. Phys. Ed.* **1995**, *33*, 2289.
(20) Liu, Z.; Kobayashi, K.; Lodge, T. P. Preprint (1996).
(21) Onuki, A.; Hashimoto, T. *Macromolecules* **1989**, *22*, 879. Hashimoto, T.; Mori, K. *Macromolecules* **1990**, *23*, 5347. Mori, K.; Okawara, A.; Hashimoto, T. *J. Chem. Phys.* **1996**, *104*, 7765.
(22) Brown, W.; Nicolai, T. *Colloid Polym. Sci.* **1990**, *268*, 977.
(23) Noda, I.; Kato, N.; Kitano, T.; Ngasawa, M. *Macromolecules* **1981**, *14*, 668.
(24) Daoud, M.; Cotton, J. P.; Farnoux, B.; Jannink, G.; Sarma, G.; Benoit, H.; Duplessix, R.; Picot, C.; DeGennes, P. G. *Macromolecules* **1975**, *8*, 804. King, J. S.; Boyer, W.; Wignall, G. D.; Ullman, R. *Macromolecules* **1985**, *18*, 709.
(25) Doi, M.; Edwards, S. F. *The Theory of Polymer Dynamics*; Oxford Science Publications, Oxford, GB, 1986.
(26) des Cloizeaux, J.; Jannink, G. *Polymer in Solution. Their Modelling and Structure*; Oxford Science Publications: Oxford, G.B., 1990.
(27) Oono, Y. *Adv. Chem. Phys.* **1985**, *61*, 301.
(28) Freed, K. F. *Renormalization Group Theory of Macromolecules*; John Wiley & Sons Inc.: New York, 1986.
(29) Fujita, H. *Polymer Solutions*; Elsevier: Amsterdam, 1990.
(30) Edwards, S. F. *J. Phys.* **1975**, *A8*, 1670. Edwards, S. F.; Jeffers, E. F. *J. Chem. Soc., Faraday Trans. 2* **1979**, *75*, 1020.
(31) Edwards, S. F. *Proc. Phys. Soc.* **1965**, *85*, 613. Muthukumar, M. *J. Chem. Phys.* **1986**, *85*, 4722.
(32) Schweizer, K. S.; Curro, J. G. *Chem. Phys.* **1990**, *149*, 105. Schweizer, K. S.; Curro, J. G. *Macromolecules* **1988**, *21*, 3070, 3082.
(33) Chandler, D. In *The Liquid State of Matter*; Montroll, E. W.; and Lebowitz, J. L., Eds.; North-Holland: Amsterdam, 1982; p 275 and references cited therein.
(34) Grayce, C. J.; Yethiraj, A.; Schweizer, K. S. *J. Chem. Phys.* **1994**, *100*, 6857.
(35) David, E. F.; Schweizer, K. S. *J. Chem. Soc., Faraday Trans.* **1995**, *91*, 2411. David, E. F.; Schweizer, K. S. *Macromolecules*, in press.
(36) Schweizer, K. S.; Honnell, K. G.; Curro, J. G. *J. Chem. Phys.* **1992**, *96*, 3211. Melenkevitz, J.; Curro, J. G.; Schweizer, K. S. *J. Chem. Phys.* **1993**, *99*, 5571.
(37) Chatterjee, A. P.; Schweizer, K. S. *Macromolecules*, submitted for publication.
(38) Schweizer, K. S.; Szamel, G. *Macromolecules* **1995**, *28*, 7543.
(39) Fetters, L. J.; Lohse, D.; Richter, D.; Witten, T.; Zirkel, A. *Macromolecules* **1994**, *22*, 4639.
(40) Schweizer, K. S.; David, E. F.; Singh, C.; Curro, J. G.; Rajasekaran, J. J. *Macromolecules* **1995**, *28*, 1528.

(41) Singh, C.; Schweizer, K. S. *Macromolecules* **1997**, *30*, 1490. Singh, C.; Schweizer, K. S. *J. Chem. Phys.* **1995**, *103*, 5814. Schweizer, K. S.; Singh, C. *Macromolecules* **1995**, *28*, 2063.

(42) Schweizer, K. S.; Yethiraj, A. *J. Chem. Phys.* **1993**, *98*, 9053. Yethiraj, A.; Schweizer, K. S. *J. Chem. Phys.* **1993**, *98*, 9080. Yethiraj, A.; Schweizer, K. S.; Singh, C. *J. Chem. Phys.* **1995**, *91*, 2411.

(43) Guenza, M.; Tang, H.; Schweizer, K. S. *Macromolecules* **1997**, *30*, 3423. Tang, H.; Schweizer, K. S. *J. Chem. Phys.* **1996**, *105*, 779. Tang, H.; Schweizer, K. S. *J. Chem. Phys.* **1995**, *103*, 6296.

(44) Matsen, M. W.; Bates, F. S. *Macromolecules* **1996**, *29*, 1091; *Macromolecules* **1995**, *28*, 8884. Matsen, M. W.; Schick, M. *Curr. Opin. Colloid Interface Sci.* **1996**, *1*, 329.

(45) Schweizer, K. S. *J. Chem. Phys.* **1989**, *91*, 5802, 5822. Schweizer, K. S.; Szamel, G. *Transp. Theory Stat. Phys.* **1995**, *24*, 947.

(46) Deutsch, H. P.; Binder, K. *Europhys. Lett.* **1992**, *17*, 697. Deutsch, H. P.; Binder, K. *J. Phys. II Fr.* **1993**, *3*, 1049. Sariban, A.; Binder, K. *Macromolecules* **1988**, *21*, 711. *Makromol. Chem.* **1988**, *189*, 2357 and references cited therein.

(47) Kolbet, K.; Schweizer, K. S. Manuscript in preparation.

(48) Fried, H.; Binder, K. *J. Chem. Phys.* **1991**, *94*, 8349. Binder, K.; Fried, H. *Macromolecules* **1993**, *26*, 6878. Weyersberg, A.; Vilgis, T. *Phys. Rev. E* **1993**, *48*, 377.

(49) Singh, C.; Schweizer, K. S. Manuscript in preparation.

(50) Schwahn, D.; Frielinghaus, H.; Mortensen, K.; Almdal, K. *Phys. Rev. Lett.* **1996**, *77*, 3153. Frielinghaus, H.; Schwahn, D.; Mortensen, K.; Almdal, K.; Springer, T. *Macromolecules* **1996**, *29*, 3263. Hajduk, D. A.; Urayama, P.; Gruner, S. M.; Erramilli, S.; Register, R. A.; Brister, K.; Fetters, L. J. *Macromolecules* **1995**, *28*, 7148. Janssen, S.; Schwahn, D.; Springer, T.; Mortensen, K. *Macromolecules* **1995**, *28*, 2555. Hammouda, B.; Bauer, B. J. *Macromolecules* **1995**, *28*, 4505.

MA970173H